Dark Matter Particle Search at Accelerators

Patkós András

Gyöngyöstarján, 2007 October

Outline

- Astrophysical evidence for DM
- Direct and indirect detection experiments
- Particle physics interpretation of $\Omega_{DM}h^2$
- Role of accelerator experiments in identifying SUSY dark matter
- Numerical simulations of typical points in the SUSY parameter space

Astrophysical evidence for DM

WMAP fit to CMB temperature fluctuation correlations (2005):

$$\Omega_{DM}h^2 = 0.105 \pm 0.013,\ h = 0.70 \pm 0.02$$

Expected accuracy of PLANCK: 0.4%

The most solid and accurate quantitative evidence for new physics

Rotation curves of galaxies (F.Zwicky, 1933):

300 times more matter than indicated by starlight,

5-10 times more than luminous matter, no more than 20% can be baryonic (MACHO) $(4 - 10 \times 10^{-25} g/cm^3)$

"Direct" photo (2006):

X-ray and gravitational lensing picture of the Bullet galaxy

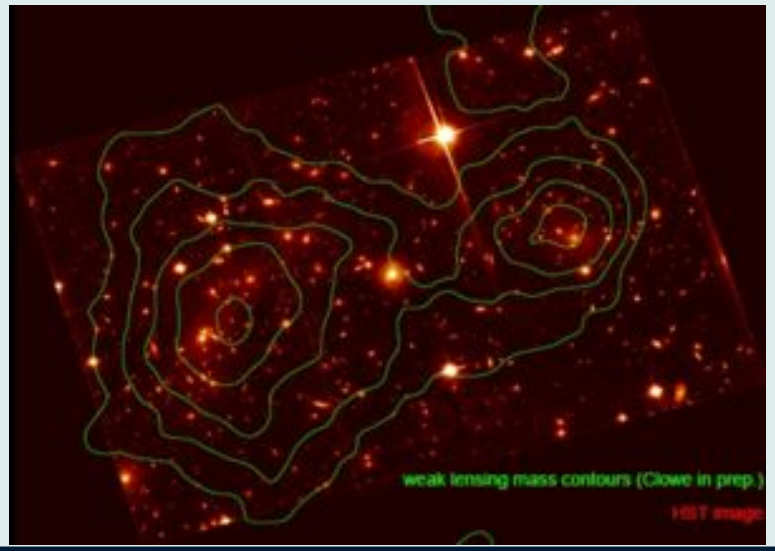

DM detection experiments I.

Direct detection: Nuclear recoil from DM-SM scattering via t-channel "light" particle (Higgs, squark, etc.) exchange

$$< E_R > \approx \frac{2v^2 m_T}{(1+m_T/m_{DM})^2}$$

Target: Xe, Ge
v DM-velocity (co-rotation with the Galaxy): 230 ± 20 km/s.

Assume $m_{DM} \approx 100$ GeV $\rightarrow \sigma \lesssim 2 \times 10^{-43}\mathrm{cm}^2$.

Theoretical problem: QCD uncertainty of Higgs-nucleon coupling (the heavier quark the stronger is the coupling):

$$\lambda_{Hpp} = \frac{m_p}{250\ GeV}\left[\frac{2}{27} + \frac{25}{27} f_{Ts}\right] \tan\beta,\ f_{Ts} = \frac{\langle p|m_s \bar{s} s|p\rangle}{\langle p|H_{QCD}|p\rangle},\ f_T = 0.36 \pm 0.14$$

Experiments: (Super)CDMS, !!DAMA: $\sigma = 5 \times 10^{-42}\mathrm{cm}^2$??,

DM detection experiments II.

Indirect detection: $\gamma, e^+, \bar{p}, \bar{D}$ from WIMP annihilation in the Galactic halo

γ-flux: $$E_\gamma \frac{d\Phi_\gamma}{dE_\gamma d\Omega} = \frac{1}{2}\langle\sigma_{ann} v\rangle \cdot \frac{E_\gamma}{\sigma_{ann}} \frac{d\sigma_{ann}}{dE_\gamma} \cdot \frac{1}{4\pi M^2_{wimp}} \times \int dz \rho(z)^2$$

$$\rho(r) = \rho_0 \left(\frac{r}{r_0}\right)^\gamma \left[\frac{1+(r_0/a)^\alpha}{1+(r/a)^\alpha}\right]^{\frac{\beta-\gamma}{\alpha}} \qquad r_0 = 8,5\text{kpc}, \rho_0 = 5.34 \times 10^{-25}\text{g/cm}^3$$

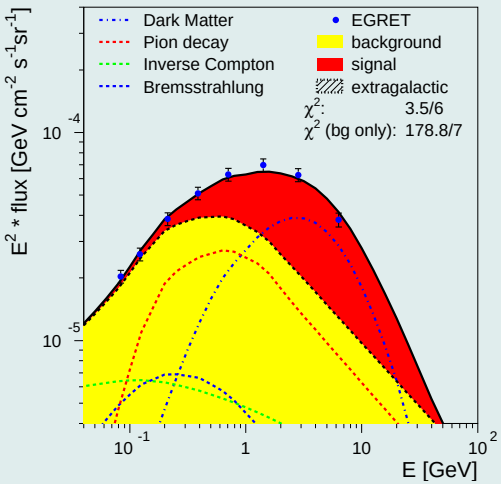

EGRET: diffuse galactic γ

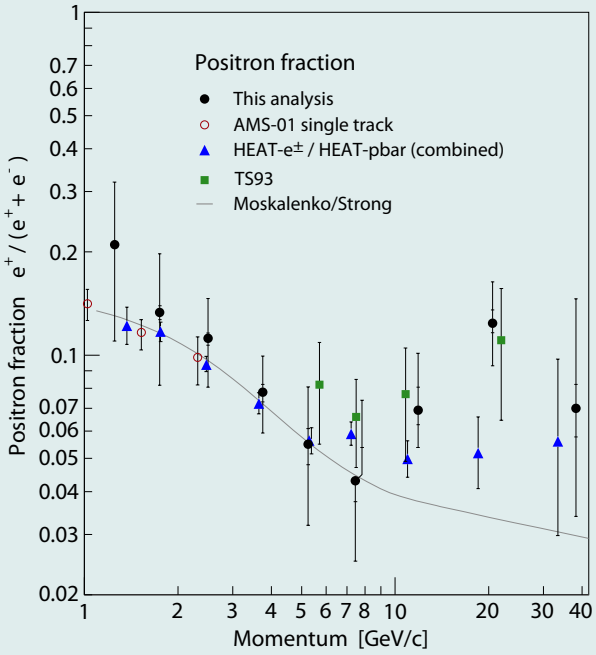

HEAT-AMS: excess e^+ yield

particle physics interpretation of $\Omega_{DM}h^2$

Semiquantitative estimate for relic dark density

Nature of stable DM-particle: self-conjugate neutral (Majorana)

DM-concentration determined by annihilation into SM-particles (lepton pairs)

Kinetic theory for isotropic and spatially homogenous single DM-particle distribution $f(\mathbf{p},t)$ in expanding universe:

$$\frac{df}{dt}=\frac{\partial f}{\partial t}-H\frac{p^2}{E}\frac{\partial f}{\partial p}, \qquad n(t)=\int_{\mathbf{p}} f(\mathbf{p},t)$$

$$\frac{dn}{dt}+3Hn(t)=\frac{1}{a(t)^3}\frac{d(na^3)}{dt}=\text{annihilation rate}$$

Annihilation rate for the $DM+DM\leftrightarrow l+\bar{l}$ type reaction:

$$\int \Pi_i \frac{d^3p_i}{(2\pi)^3} \qquad (2\pi)^4\delta^{(4)}(\sum p_i)|M_{fi}|^2$$

$$\times\left(f_l f_{\bar{l}}(1\pm f_{DM})(1\pm f_{DM'})-f_{DM}f'_{DM}(1\pm f_l)(1\pm f_{\bar{l}})\right).$$

particle physics interpretation of $\Omega_{DM}h^2$

For nonrelativistic DM-particles ($T/M_{DM} \sim 1/25$) use of Boltzmann-distribution is legitimate $\rightarrow$ exponentially small DM-density:

$$n_i(t) = n_i^0 e^{-E_i/T} \times e^{\mu_i/T}, f_i << 1.$$

Relativistic SM-particle density is not influenced by this reaction:
$n_l(t) = n_l^0, n_{\bar{l}} = n_{\bar{l}}^0$

$$\text{annihilation rate} = (n_{DM}^0)^2 \overline{\sigma_{ann} v_{DM}}^T \left[1 - \left(\frac{n_{DM}(t)}{n_{DM}^0}\right)^2\right],$$

with termally averaged transition matrix element:

$$\overline{\sigma_{ann} v_{DM}}^T = \int \Pi_i \frac{d^3 p_i}{(2\pi)^3} (2\pi)^4 \delta^{(4)}(\sum p_i) e^{-E_{tot}/T} |M_{fi}|^2.$$

Numerical integration of rate equation shows decoupling for $T \sim M_{DM}/25$.

$$\Omega_{DM}h^2 = \frac{s_0}{\rho_c} h^2 \left(\frac{45}{\pi g_*}\right)^{1/2} \frac{25}{M_{Pl}} \frac{1}{\langle \sigma v \rangle}, \qquad \Omega_{DM} \approx 0.2 \rightarrow \langle \sigma v \rangle \approx 10^{-36} \text{cm}^3/s.$$

particle physics interpretation of $\Omega_{DM}h^2$

Typical BSM theory: Nearby excitations to the Lightest "Stable" BSM Particle.

Edsjö, Gondolo (1997): Important co-annihilation processes in SUSY

Initial state	Final state	Feynman diagrams
$\chi_i^0\chi_j^0$	$H_1H_1,\ H_1H_2,\ H_2H_2,\ H_3H_3$	$t(\chi_k^0),\ u(\chi_k^0),\ s(H_{1,2})$
	$H_1H_3,\ H_2H_3$	$t(\chi_k^0),\ u(\chi_k^0),\ s(H_3),\ s(Z^0)$
	H^-H^+	$t(\chi_e^+),\ u(\chi_e^+),\ s(H_{1,2}),\ s(Z^0)$
	$Z^0H_1,\ Z^0H_2$	$t(\chi_k^0),\ u(\chi_k^0),\ s(H_3),\ s(Z^0)$
	Z^0H_3	$t(\chi_k^0),\ u(\chi_k^0),\ s(H_{1,2})$
	$W^-H^+,\ W^+H^-$	$t(\chi_e^+),\ u(\chi_e^+),\ s(H_{1,2,3})$
	Z^0Z^0	$t(\chi_k^0),\ u(\chi_k^0),\ s(H_{1,2})$
	W^-W^+	$t(\chi_e^+),\ u(\chi_e^+),\ s(H_{1,2}),\ s(Z^0)$
	$f\bar{f}$	$t(\tilde{f}_{L,R}),\ u(\tilde{f}_{L,R}),\ s(H_{1,2,3}),\ s(Z^0)$

particle physics interpretation of $\Omega_{DM}h^2$

Initial state	Final state	Feynman diagrams
$\chi_c^+\chi_i^0$	H^+H_1, H^+H_2	$t(\chi_k^0)$, $u(\chi_e^+)$, $s(H^+)$, $s(W^+)$
	H^+H_3	$t(\chi_k^0)$, $u(\chi_e^+)$, $s(W^+)$
	W^+H_1, W^+H_2	$t(\chi_k^0)$, $u(\chi_e^+)$, $s(H^+)$, $s(W^+)$
	W^+H_3	$t(\chi_k^0)$, $u(\chi_e^+)$, $s(H^+)$
	H^+Z^0	$t(\chi_k^0)$, $u(\chi_e^+)$, $s(H^+)$
	γH^+	$t(\chi_c^+)$, $s(H^+)$
	W^+Z^0	$t(\chi_k^0)$, $u(\chi_e^+)$, $s(W^+)$
	γW^+	$t(\chi_c^+)$, $s(W^+)$
	$u\bar{d}$	$t(\tilde{d}_{L,R})$, $u(\tilde{u}_{L,R})$, $s(H^+)$, $s(W^+)$
	$\nu\bar{\ell}$	$t(\tilde{\ell}_{L,R})$, $u(\tilde{\nu}_L)$, $s(H^+)$, $s(W^+)$
$\chi_c^+\chi_d^+$	H^+H^+	$t(\chi_k^0)$, $u(\chi_k^0)$
	H^+W^+	$t(\chi_k^0)$, $u(\chi_k^0)$
	W^+W^+	$t(\chi_k^0)$, $u(\chi_k^0)$

particle physics interpretation of $\Omega_{DM}h^2$

Initial state	Final state	Feynman diagrams
	H_1H_1, H_1H_2, H_2H_2, H_3H_3	$t(\chi_e^+)$, $u(\chi_e^+)$, $s(H_{1,2})$
	H_1H_3, H_2H_3	$t(\chi_e^+)$, $u(\chi_e^+)$, $s(H_3)$, $s(Z^0)$
	H^+H^-	$t(\chi_k^0)$, $s(H_{1,2})$, $s(Z^0,\gamma)$
	Z^0H_1, Z^0H_2	$t(\chi_e^+)$, $u(\chi_e^+)$, $s(H_3)$, $s(Z^0)$
	Z^0H_3	$t(\chi_e^+)$, $u(\chi_e^+)$, $s(H_{1,2})$
	H^+W^-, W^+H^-	$t(\chi_e^+)$, $s(H_{1,2,3})$
$\chi_c^+\chi_d^-$	Z^0Z^0	$t(\chi_e^+)$, $u(\chi_e^+)$, $s(H_{1,2})$
	W^+W^-	$t(\chi_k^0)$, $s(H_{1,2})$, $s(Z^0,\gamma)$
	$\gamma\gamma$ (only for $c=d$)	$t(\chi_c^+)$, $u(\chi_c^+)$
	$Z^0\gamma$	$t(\chi_d^+)$, $u(\chi_c^+)$
	$u\bar{u}$	$t(\tilde{d}_{L,R})$, $s(H_{1,2,3})$, $s(Z^0,\gamma)$
	$\nu\bar{\nu}$	$t(\tilde{\ell}_{L,R})$, $s(Z^0)$
	$\bar{d}d$	$t(\tilde{u}_{L,R})$, $s(H_{1,2,3})$, $s(Z^0,\gamma)$
	$\bar{\ell}\ell$	$t(\tilde{\nu}_L)$, $s(H_{1,2,3})$, $s(Z^0,\gamma)$

particle physics interpretation of $\Omega_{DM}h^2$

The complete reaction network:

$$\begin{aligned}
\frac{dn_i}{dt} &= -3Hn_i - \sum_{j=1}^{N} \langle \sigma_{ij} v_{ij} \rangle \left(n_i n_j - n_i^0 n_j^0 \right) \\
&\quad - \sum_{j \neq i} \left[\langle \sigma'_{X ij} v_{ij} \rangle \left(n_i n_X - n_i^0 n_X^0 \right) - \langle \sigma'_{X ji} v_{ij} \rangle \left(n_j n_X - n_j^0 n_X^0 \right) \right] \\
&\quad - \sum_{j \neq i} \left[\Gamma_{ij} \left(n_i - n_i^0 \right) - \Gamma_{ji} \left(n_j - n_j^0 \right) \right].
\end{aligned}$$

Second term: $\chi_i \chi_j$ annihilations with total annihilation cross section:

$$\sigma_{ij} = \sum_X \sigma(\chi_i \chi_j \to X).$$

Third term: $\chi_i \to \chi_j$ scattering off the cosmic thermal background,

$$\sigma'_{X ij} = \sum_Y \sigma(\chi_i X \to \chi_j Y)$$

particle physics interpretation of $\Omega_{DM}h^2$

Fourth term: χ_i decays

$$\Gamma_{ij} \quad = \quad \sum_X \Gamma(\chi_i \to \chi_j X).$$

Thermal average computed in equilibrium:

$$\langle \sigma_{ij} v_{ij} \rangle \quad = \quad \frac{\int d^3\mathbf{p}_i d^3\mathbf{p}_j f_i f_j \sigma_{ij} v_{ij}}{\int d^3\mathbf{p}_i d^3\mathbf{p}_j f_i f_j}, \qquad v_{ij} = \frac{\sqrt{(p_i \cdot p_j)^2 - m_i^2 m_j^2}}{E_i E_j}$$

"Practical" (R-parity) conservation: all particles decay into the lightest one.
Final abundance: sum of the densities of all BSM-particles,

$$n = \sum_{i=1}^{N} n_i, \qquad \frac{dn}{dt} \quad = \quad -3Hn - \sum_{i,j=1}^{N} \langle \sigma_{ij} v_{ij} \rangle \left(n_i n_j - n_i^0 n_j^0 \right)$$

particle physics interpretation of $\Omega_{DM}h^2$

Background density (n_X) is much larger than the Boltzmann-suppressed DM-density (n_i).

$DM_i + X \to DM_j + Y$ keeps DM in thermal equilibrium: $\frac{n_i}{n} = \frac{n_i^0}{n^0}$.

$$\frac{dn}{dt} = -3Hn - \langle\sigma_{\rm eff} v\rangle \left(n^2 - (n^0)^2\right), \qquad \langle\sigma_{\rm eff} v\rangle = \sum_{ij} \langle\sigma_{ij} v_{ij}\rangle \frac{n_i^0}{n^0}\frac{n_j^0}{n^0}.$$

For integration introduce $Y = n/s$ and $x = M_{MD}/T$:

$$\frac{dY}{dx} = -\sqrt{\frac{\pi}{45G}} \frac{g_*^{1/2} M_{DM}}{x^2} \langle\sigma_{eff} v\rangle (Y^2 - Y_0^2),$$

$$Y_0 = \frac{45x^2}{4\pi^4 h_{eff}(T)} \sum_i g_i \left(\frac{m_i}{M_{DM}}\right)^2 K_2\left(x\frac{m_i}{M_{DM}}\right), \qquad s = h_{eff}(T)\frac{2\pi^2}{45}T^3.$$

particle physics interpretation of $\Omega_{DM}h^2$

Astro-particle physics literature on DM:

D. Hooper: Indirect Searches for Dark Matter (arxiv:0710.2062, hep-ph)

E.W. Kolb and M.S. Turner: The Early Universe (Ch. 5.2 Freeze out)

Frei Zs., Patkós A.: Inflációs kozmológia (6.3 fejezet)

J. Edsjö and P. Gondolo: Neutralino Relic Density Including Coannihilations, Phys. Rev. **D56**, 1879 (1997)

P. Gondolo, J. Edsjö, P. Ullio, L. Bergström, M.Schelke and E.A. Baltz: DarkSUSY: Computing Supersymmetric Dark Matter Propoerties Numerically astro-ph/0406204 (2004 June)

Accelerator exploration of SUSY DM particle

Discussion follows: E.M. Baltz, M. Battaglia, M.E. Peskin and T. Wizansky:

Determination of Dark Matter Properties at High Energy Collisions

Phys. Rev. **D74** 103521 (2006)

Non-trivial question: To what accuracy can one prove that the particle(s) to be discovered by missing energy analysis at LHC (ILC) is identical to the WIMP constituent of DM?

Proposed strategy:

1. Mass spectra estimates at LHC, ILC
2. Direct detection at CDMS, SuperCDMS

$\rightarrow$ Data sufficient for fixing theoretical framework

3. Relic density calculation from the model
4. Direct and indirect detection cross-section estimates from the model
5. Reconstruction of the galactic DM-profile

Choosing typical points to simulate the strategy

108 MSSM SUSY parameters

FCNC suppression, CP-conservation: 24 parameters

$M_i, \mu, \quad i = 1, 2, 3$ gaugino, Higgsino mass parameters

$M^2(L_i), M^2(\tilde{e}_i), \quad i = 1, 2, 3$ slepton masses

$M^2(Q_i), M^2(\tilde{u}_i), M^2(\tilde{d}_i), \quad i, 1, 2, 3$ squark masses

$m_A, \tan\beta \leftrightarrow m_1, m_2$ Higgs potential parameters

A_E, A_D, A_U trilinear couplings

The soft supersymmetry-breaking potential

$$V_{\text{soft}} = \epsilon_{ij}\left(\tilde{\mathbf{e}}^*_R \mathbf{A}_E \mathbf{Y}_E \tilde{\mathbf{l}}^i_L H^j_1 + \tilde{\mathbf{d}}^*_R \mathbf{A}_D \mathbf{Y}_D \tilde{\mathbf{q}}^i_L H^j_1 - \tilde{\mathbf{u}}^*_R \mathbf{A}_U \mathbf{Y}_U \tilde{\mathbf{q}}^i_L H^j_2\right)$$

$$-\epsilon_{ij} B\mu H^i_1 H^j_2 + H^{i*}_1 m^2_1 H^i_1 + H^{i*}_2 m^2_2 H^i_2$$

$$+\tilde{\mathbf{q}}^{i*}_L \mathbf{M}^2_Q \tilde{\mathbf{q}}^i_L + \tilde{\mathbf{l}}^{i*}_L \mathbf{M}^2_L \tilde{\mathbf{l}}^i_L + \tilde{\mathbf{u}}^*_R \mathbf{M}^2_U \tilde{\mathbf{u}}_R + \tilde{\mathbf{d}}^*_R \mathbf{M}^2_D \tilde{\mathbf{d}}_R + \tilde{\mathbf{e}}^*_R \mathbf{M}^2_E \tilde{\mathbf{e}}_R$$

$$+\tfrac{1}{2} M_1 \tilde{B}\tilde{B} + \tfrac{1}{2} M_2 \left(\tilde{W}^3 \tilde{W}^3 + 2\tilde{W}^+ \tilde{W}^-\right) + \tfrac{1}{2} M_3 \tilde{g}\tilde{g}.$$

Choosing typical points to simulate the strategy

Further artificial reduction: $m_0, m_{1/2}, A_0, \mu/|\mu|, m_t, \tan\beta$ "mSUGRA"

Points with characteristically different annihilation channels are chosen

Point	m_0	$m_{1/2}$	$\tan\beta$	A_0	$\mu/\|\mu\|$	m_t	$\Omega_\chi h^2$	
LCC1	100	250	10	-100	$+$	175	0.192	$l\bar{l}$
LCC2	3280	300	10	0	$+$	175	0.109	W^+W^-
LCC3	213	360	40	0	$+$	175	0.101	coann
LCC4	380	420	53	0	$+$	178	0.114	$b\bar{b}$
SPS1a′	70	250	10	-300	$+$	175	0.115	

Spectrum and neutralino, chargino mixing angle calculation:
ISAJET 7.68 package (F. Paige *et al.* hep-ph/0312045) – 1-loop level mass matrix

Relic density + neutralino d+id detection Xsections:
DarkSUSY-4.1 – tree level

Exploring the 24 dimensional neighbourhood of the selected point

Markov Chain Monte Carlo in the parameter space starting from the chosen "mSUGRA" point:

Define likelihood function L in the parameter space with some *a priori* form (somewhat arbitrary e.g dm/m distribution for mass-parameters, etc.).

Vary 24(!) parameters and accept the new point, if $L_{new} > L_{old}$ and with probability L_{new}/L_{old}, if $L_{new} < L_{old}$.
Implement importance sampling in Ω_χ^2 around the WMAP-value with 3% normal deviation.

25 independent chains, each 160000 points

Calculate spectra, Xsections accessible for LHC, ILC500, ILC100 and use them for the determination of astrophysical observables $\Omega_\chi h^2$, d+id detection cross sections.

Present the probability distribution of these observables for the generated ensemble.

LCC1

Spectral characterisation

$\tilde{\chi}_1^0$ mostly *bino*: annihilation into lepton pairs; no W^+W^-, Z^0Z^0 production

light sleptons dominate annihilation: accurate knowledge of $m(\tilde{l})$ is needed for accurate prediction for $\Omega_\chi h^2$

$m(\tilde{q}_R)$ determination from direct decay into χ_1^0; large BR of $\tilde{q}_L$ into $\tilde{\chi}_2^0$.

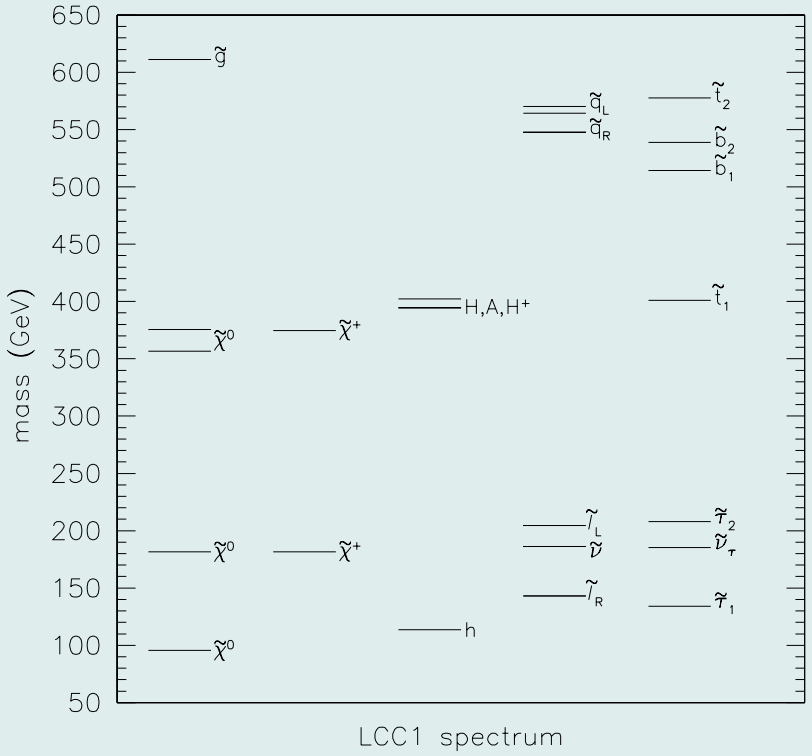

LCC1

Accurate LHC determination of mass differences by kinematical end-points of the lepton energy in two-body decays: $\tilde{\chi}_2^0 \to \tilde{l}l, \tilde{l} \to \tilde{\chi}_1^0 l$.

Overconstrained ll-spectra: also $\tilde{l}$ masses can be determined.

mass/mass splitting	LCC1 Value		LHC	ILC 500	ILC 1000
$m(\tilde{\chi}_1^0)$	95.5	$\pm$	4.8	0.05	
$m(\tilde{\chi}_2^0) - m(\tilde{\chi}_1^0)$	86.1	$\pm$	1.2	0.07	
$m(\tilde{\chi}_3^0) - m(\tilde{\chi}_1^0)$	261.2	$\pm$	@^{a}	4.0	
$m(\tilde{\chi}_4^0) - m(\tilde{\chi}_1^0)$	280.1	$\pm$	2.2^a	2.2	
$m(\tilde{\chi}_1^+)$	181.7	$\pm$	-	0.55	
$m(\tilde{\chi}_2^+)$	374.7	$\pm$	-	-	3.0
$m(\tilde{e}_R)$	143.1	$\pm$	-	0.05	
$m(\tilde{e}_R) - m(\tilde{\chi}_1^0)$	47.6	$\pm$	1.0	0.2	
$m(\tilde{\mu}_R) - m(\tilde{\chi}_1^0)$	47.5	$\pm$	1.0	0.2	
$m(\tilde{\tau}_1) - m(\tilde{\chi}_1^0)$	38.6	$\pm$	5.0	0.3	
$BR(\tilde{\chi}_2^0 \to \tilde{e}e)/BR(\tilde{\chi}_2^0 \to \tilde{\tau}\tau)$	0.077	$\pm$	0.008		
$m(\tilde{e}_L) - m(\tilde{\chi}_1^0)$	109.1	$\pm$	1.2	0.2	
$m(\tilde{\mu}_L) - m(\tilde{\chi}_1^0)$	109.1	$\pm$	1.2	1.0	
$m(\tilde{\tau}_2) - m(\tilde{\chi}_1^0)$	112.3	$\pm$	-	1.1	
$m(\tilde{\nu}_e)$	186.2	$\pm$	-	1.2	

LCC1

mass/mass splitting	LCC1 Value		LHC	ILC 500	ILC 1000
$m(h)$	113.68	$\pm$	0.25	0.05	
$m(A)$	394.4	$\pm$	*	(> 240)	1.5
$m(\tilde{u}_R)$, $m(\tilde{d}_R)$	548.	$\pm$	19.0	16.0	
$m(\tilde{s}_R)$, $m(\tilde{c}_R)$	548.	$\pm$	19.0	16.0	
$m(\tilde{u}_L)$, $m(\tilde{d}_L)$	564., 570.	$\pm$	17.4	9.8	
$m(\tilde{s}_L)$, $m(\tilde{c}_L)$	570., 564.	$\pm$	17.4	9.8	
$m(\tilde{b}_1)$	514.	$\pm$	7.5	5.7	
$m(\tilde{b}_2)$	539.	$\pm$	7.9	6.2	
$m(\tilde{t}_1)$	401.	$\pm$	(> 270)	-	2.0
$m(\tilde{g})$	611.	$\pm$	8.0	6.5	

ILC-1000 can access also $\tilde{t}_1\bar{\tilde{t}}_1$ production. From threshold energy determination absolute mass determinations are possible.

ILC-500 determines X-sections for $e^+e^- \to \tilde{\chi}_i^0\tilde{\chi}_j^0, \tilde{\chi}^+\tilde{\chi}^-, \tilde{\tau}^+\tilde{\tau}^-, \tilde{e}_R^+\tilde{e}_R^-$.

LCC1

LHC estimate of $\Omega_\chi h^2$ is limited by the inaccuracy of absolute mass determination to cca. 7%. ILC-1000: 0.25% comparable to PLANCK.

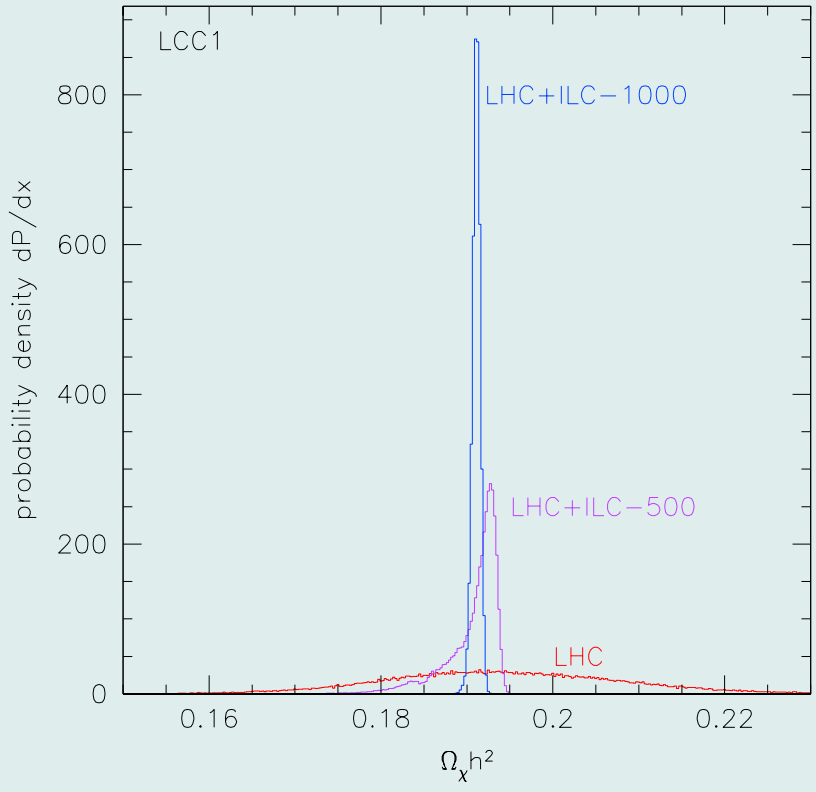

LCC1

Direct detection: dominated by heavy H^0 exchange
ILC-1000 will access $e^+e^- \to H^0A^0$ enabling more accurate determination direct detection Xsection.

Near-threshold annihilation (indirect detection): sharp lines in γ spectra from exclusive $\gamma\gamma$ and γZ^0 decays

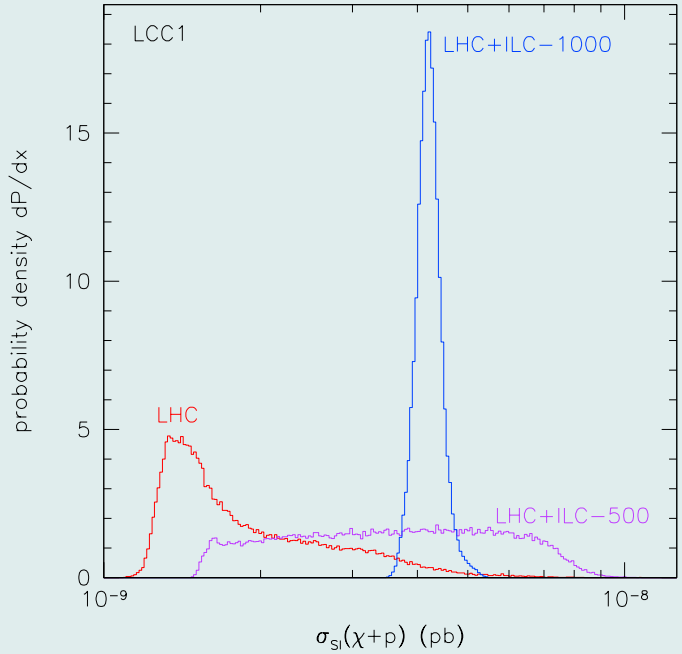

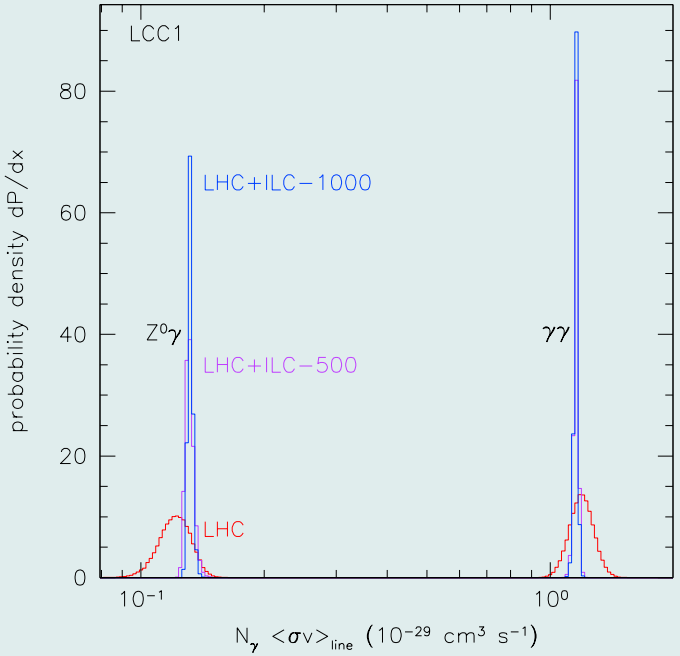

γ radiation in DM annihilation

T.Bringman, L. Bergström, J. Edsjö (2007 Oct.):
internal bremsstrahlung from charged final/virtual particles:

$$\frac{dN^{\gamma,\mathrm{tot}}}{dx} = \sum_f B_f \left(\frac{dN_f^{\gamma,\mathrm{sec}}}{dx} + \frac{dN_f^{\gamma,\mathrm{IB}}}{dx} + \frac{dN_f^{\gamma,\mathrm{line}}}{dx} \right), \quad x = E_\gamma / m_\chi$$

$$\frac{dN_{X\bar{X}}}{dx} \equiv \frac{1}{\sigma_{\chi\chi\to X\bar{X}}} \frac{d\sigma_{\chi\chi\to X\bar{X}\gamma}}{dx}$$

First term: γ-radiation from decaying annihilation products (mainly π^0), called secondary photons
Second term: internal bremsstrahlung

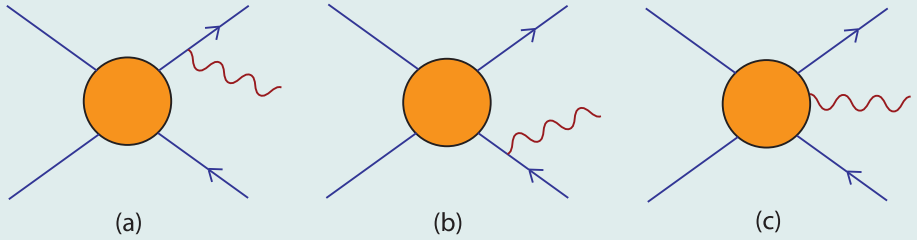

Third term: direct annihilation into $\gamma\gamma$ and γZ^0 (discrete lines)
Most important IB-channels: $W^\pm H^\mp \gamma$, $W^+W^-\gamma$, $H^+H^-\gamma$ and $f\bar{f}\gamma$

γ radiation in DM annihilation

Hard γ radiation dominates
Zero velocity limit: H^+H^- is forbidden by CP, $f\bar{f}$ is suppressed by $(m_f/m_\chi)^2$, but no restriction if extra γ is radiated!
MSSM models (7 dimensional space): $\mu; \tan\beta; M_1 \approx M_2/2, M_3; m_0, A_t, A_b$
MCMC model sequence:
200.000 models obeying WMAP bound, and accelerator constraints
Typical values

$$\frac{IB}{\gamma\gamma + \gamma Z^0} \sim 2 - 9$$

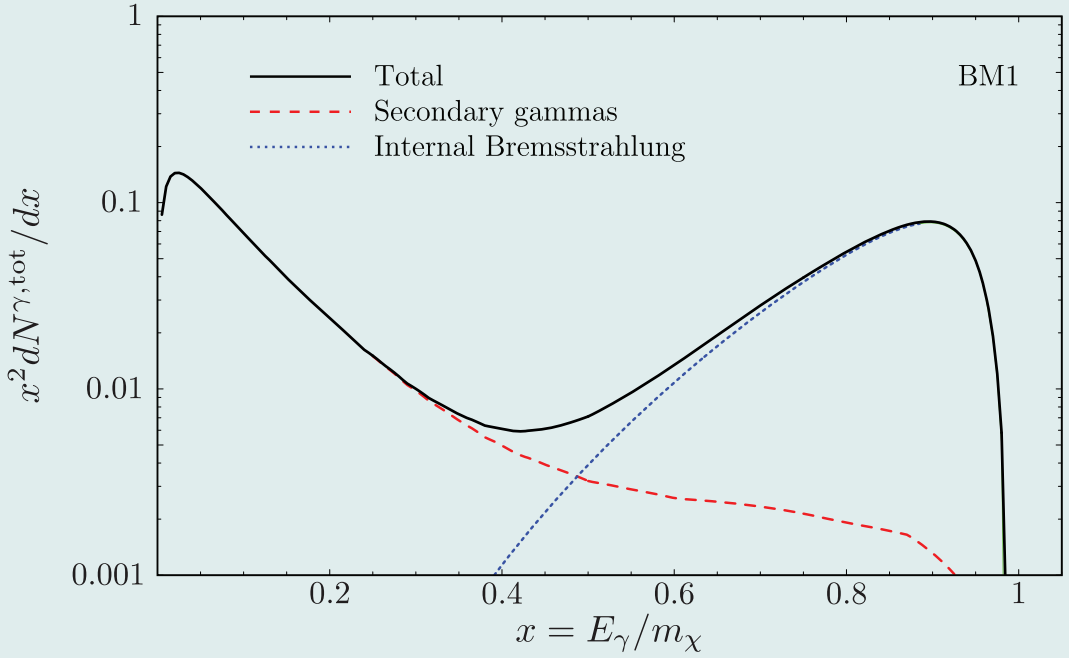

LCC2

LCC1: maximal number of SUSY particles observable at LHC

LCC2:

$\tilde{q}, \tilde{l}$ are very heavy;

$m(\tilde{\chi}^0), m(\tilde{\chi}^+) \sim 100 - 300\mathrm{GeV}$

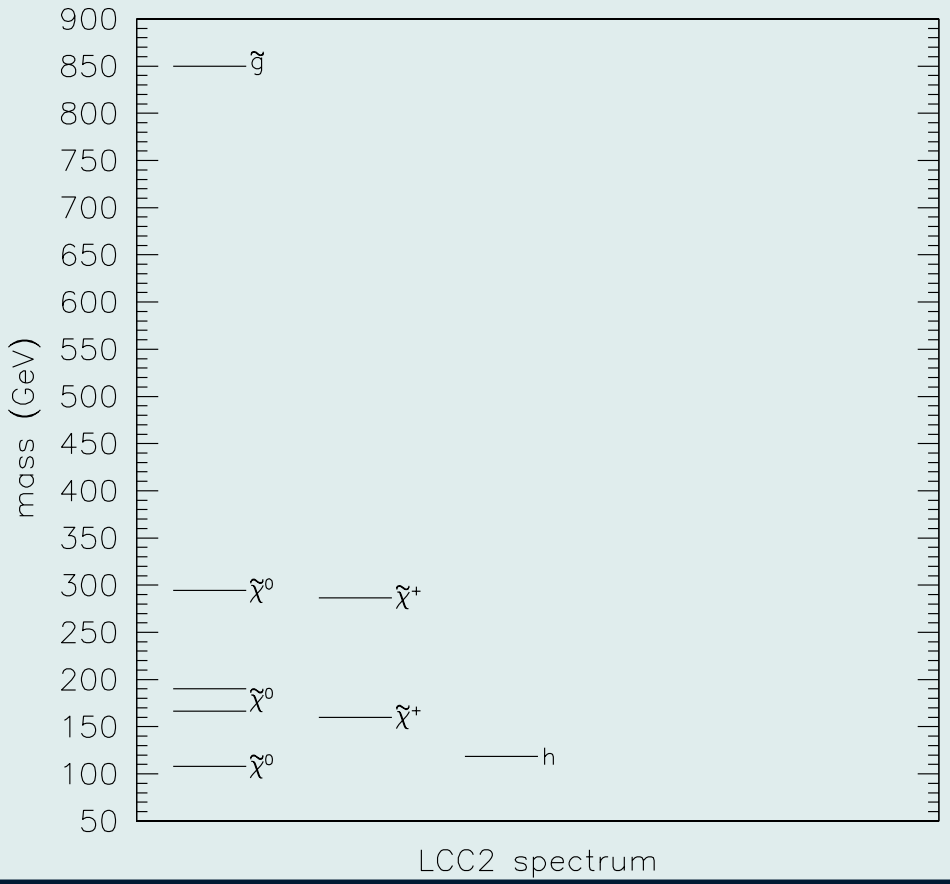

LCC2

LHC events produce $\tilde{g}$-pairs decaying into $q\bar{q}\chi$

Excited χ decays with lepton pairs into LSP

10% accurate mass determinations but no information for charginos

ILC500: $e^-e^+ \to \tilde{\chi}^-\tilde{\chi}^+, \chi_2^0\chi_3^0$

ILC1000: pair production of higher neutralinos and charginos

mass/mass splitting	LCC2 value		LHC	ILC 500	ILC 1000
$m(\tilde{\chi}_1^0)$	107.9	$\pm$	10	1.0	
$m(\tilde{\chi}_2^0) - m(\tilde{\chi}_1^0)$	58.5	$\pm$	1.0	0.3	
$m(\tilde{\chi}_3^0) - m(\tilde{\chi}_1^0)$	82.3	$\pm$	1.0	0.2	
$m(\tilde{\chi}_4^0) - m(\tilde{\chi}_1^0)$	186.3	$\pm$	-	-	3.0
$m(\tilde{\chi}_1^+)$	159.7	$\pm$	-	0.55	
$m(\tilde{\chi}_1^+) - m(\tilde{\chi}_1^0)$	51.8	$\pm$	-	0.25	
$m(\tilde{\chi}_2^+)$	286.7	$\pm$	-	-	1.0
$m(h)$	118.68	$\pm$	0.25	0.05	
$m(A)$	3242.	$\pm$	*	(> 240)	(> 480)
$m(\tilde{g})$	850.	$\pm$	85.		

LCC2

Relic density determinations: LHC $\sim 40\%$, ILC500 $\sim 14\%$, ILC100 $\sim 8\%$
Source of inaccuracies: insufficient determination of the gaugino-Higgsino mixing (bino, wino, higgsino dominated solutions found for the same LHC data!)
e^+e^- data added: wino, Higgsino dominated data give too low $\Omega_\chi h^2$, can be excluded (1-5% accuracy, sensitivity to gaugino-higgsino mixing)

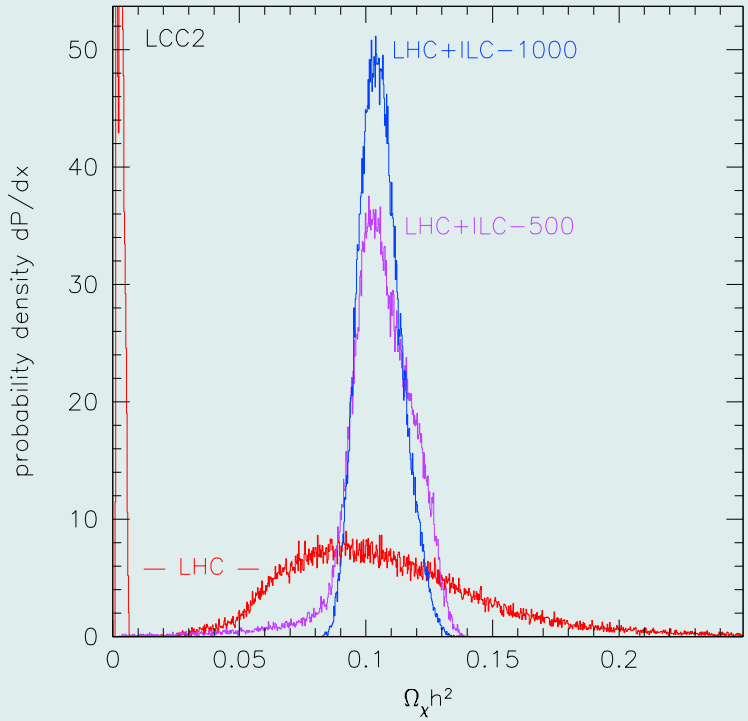

LCC2

Annihilation Xsection at threshold and at freeze out are similar:
low $\Omega_\chi h^2$ is equivalent to efficient annihilation
reflected also in direct $\gamma\gamma + \gamma Z^0$: 50 times larger yield than at LCC1 $\rightarrow$ GLAST signal!

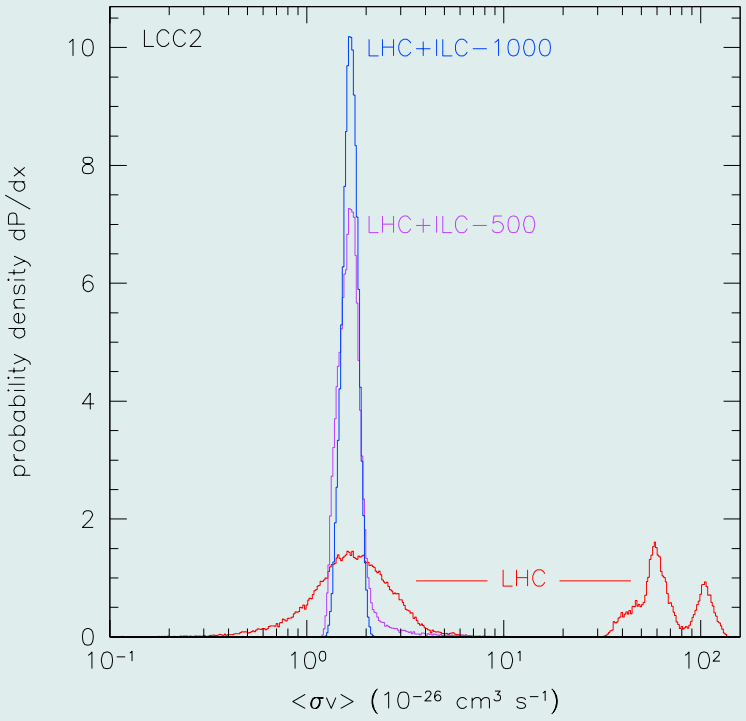

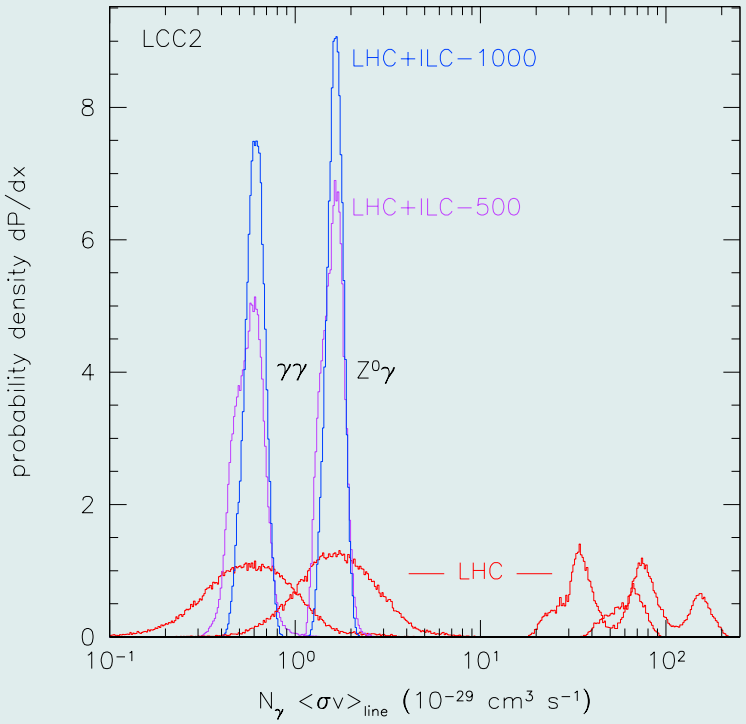

LCC2

Direct detection dominated by the t-channel exchange of h^0.
Mass determination from $h^0 \longrightarrow \gamma\gamma$
High Xsection values will be disqualified by ILC

Combined with SuperCDMS: effective local halo flux will be estimated

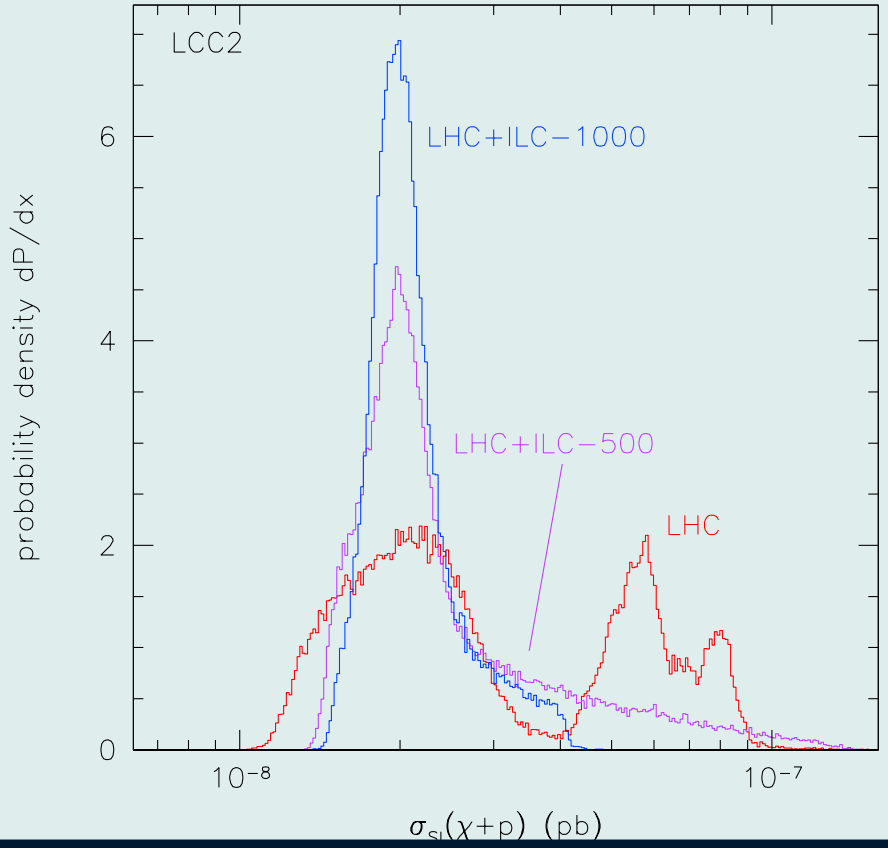

CONCLUSIONS

1. LHC might be able to identify regions of the MSSM parameter space best interpreting the missing energy data and corresponding to characteristically different annihilation mechanisms.

2. LHC can restrict only under very fortunate circumstances Ω_χ competitive with CMB observation.

3. ILC and d&id observations are needed to pin down the parameters of the qualitatively determined SUSY model

4. It would be interesting to see other candidate explanations of missing energy (Xtra dim, extended Higgs sector, etc.) analysed with similar attitude